THE JOURNAL OF PHYSICAL CHEMISTRY A

Article

pubs.acs.org/JPCA

Trans−Cis Isomerization of Vinylketones through Triplet 1,2-Biradicals

R. A. A. Upul Ranaweera,[†] Tianeka Scott,[†] Qian Li,[†] Sridhar Rajam,[†] Alexander Duncan,[†] Rui Li,[‡] Anthony Evans,[§] Cornelia Bohne,[‡] John P. Toscano,[§] Bruce S. Ault,[†] and Anna D. Gudmundsdottir*,[†]

[†]Department of Chemistry, University of Cincinnati, Cincinnati, Ohio 45221, United States

[‡]Department of Chemistry, University of Victoria, Victoria, BC V8P 5C2, Canada

[§]Department of Chemistry, John Hopkins University, Baltimore, Maryland 21218, United States

Supporting Information

ABSTRACT: The irradiation of *trans*-vinylketones **1a−c** yields the corresponding cis isomers **2a−c**. Laser flash photolysis of **1a** and **1b** with 308 and 355 nm lasers results in their triplet ketones (T_{1K} of **1**), which rearrange to form triplet 1,2-biradicals **3a** and **3b**, respectively, whereas irradiation with a 266 nm laser produces their cis-isomers through singlet reactivity. Time-resolved IR spectroscopy of **1a** with 266 nm irradiation confirmed that **2a** is formed within the laser pulse. In comparison, laser flash photolysis of **1c** with a 308 nm laser showed only the formation of **2c** through singlet reactivity. At cryogenic temperatures, the irradiation of **1** also resulted in **2**. DFT calculations were used to aid in the characterization of the excited states and biradicals involved in the cis−trans isomerization and to support the mechanism for the cis−trans isomerization on the triplet surface.

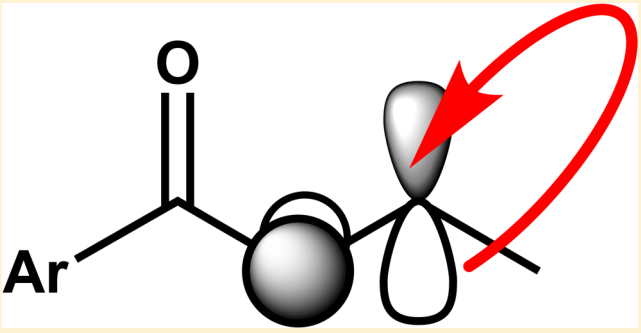

1. INTRODUCTION

The cis−trans isomerization of alkenes has potential applications in light-triggered photoswitches, photoremovable protecting groups, and image storage devices, and these applications are of general interest.[1,2] In the 1970s, Mulliken suggested that the cis−trans isomerization of ethylene on the triplet surface takes place via a twisted 1,2-biradical intermediate, $^*P^3$, known as the phantom state.[3,4] The twisted geometry of the 1,2-biradical offsets the electronic repulsion between the unpaired electrons on the adjacent carbon atoms. *Ab initio* theory studies predict the energy gap between the ground state and the $^*P^3$ of ethylene to be ∼60 kcal/mol. Only recently has laser flash photolysis revealed the property of S_1 of ethylene to have a lifetime of less than 200 fs.[5,6] Intersystem crossing to $^*P^3$ of ethylene was not observed, but internal conversion to S_0 occurred instead.

Despite the importance of cis−trans isomerization, simple 1,2-biradicals have been studied sporadically because the direct irradiation of simple alkenes does not result in intersystem crossing to their triplet surface.[7,8] In comparison, the cis−trans isomerization of styrene on its singlet and triplet surface has been studied extensively.[9−18] For example, Caldwell et al. have shown that triplet-sensitized photolysis of styrene derivatives results in triplet 1,2-biradicals. The lifetimes of acyclic flexible 1,2-biradicals were found to be within ∼100 ns, whereas for rigid or cyclic styrene derivatives, which have limited rotation, the lifetimes increased to a few microseconds.[9]

More recently, Garcia-Exposito et al. studied intermolecular photosensitization of 2-pentenoate esters and found that they formed long-lived triplet 1,2-biradicals (Scheme 1).[19] The authors explained that these biradicals are long-lived because the decay from the triplet to the singlet surface is enhanced by spin−orbit coupling[20] which is negligible in the minimal energy conformer of the 1,2-biradicals. The large energy gap between the singlet and triplet surfaces restricts efficient intersystem crossing, and although the energy gap is at minimum in the minimal energy conformer of the 1,2-biradical, it was theorized that the intersystem crossing from the triplet surface to the singlet one takes place where the two 1,2-biradicals centers are located ∼45° apart, where the spin−orbit coupling is more significant. Caldwell and co-workers came to a similar conclusion for the spin−orbit coupling in ethylene.[21]

In this paper, we report the photochemistry of simple alkenes **1** that have a built-in intramolecular sensitizer. The photochemistry of **1a** and **1b** is wavelength dependent, as laser flash photolysis of them with 355 and 308 nm lasers allowed us to detect both triplet 1,2-biradicals and their triplet ketone precursors. The biradicals have a lifetime of ∼3−6 μs in acetonitrile and reacted with O_2 with a rate constant of the

Special Issue: Current Topics in Photochemistry

Received: April 29, 2014
Revised: June 29, 2014
Published: July 2, 2014

Scheme 1

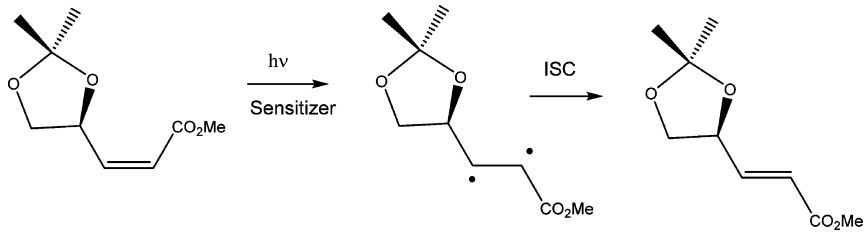

Scheme 2. Product Studies of 1a−c

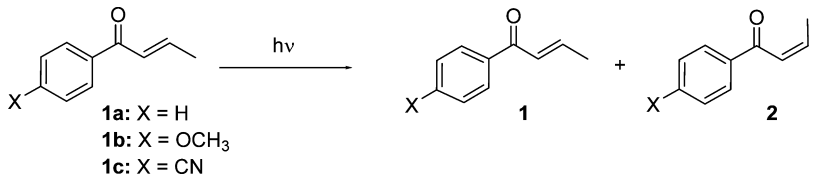

order of 10^9 M^{-1} s^{-1}. The mechanism for the cis−trans isomerization on the triplet surface was supported with density functional theory calculations. In comparison, laser flash photolysis of **1a** and **1b** with 266 nm laser results in cis−trans isomerization on the singlet surface as no triplet transients were detected.

2. RESULTS

2.1. Product Studies. Photolysis of **1a−c** in argon-saturated chloroform-*d* through a Pyrex filter (>300 nm) at 298 K yielded **2a−c** as the only products (Scheme 2, Table 1).

Table 1. Percent Conversion of 1 into 2 upon Irradiation through Pyrex (>300 nm) in $CDCl_3$[a]

compound	atmosphere	product ratio 1:2[b]	
1a[b]	Ar	67	33
	O_2	74	26
1b[b]	Ar	55	45
	O_2	68	29
1c	Ar	95	5
	O_2	94	4

[a]**2a**, **2b**, and **2c** are stable at room temperature for more than 7 days. [b]From ^{1}H NMR integration (±1%).

It should be noted that cis **2a**, **2b**, and **2c** were stable in solution and did not revert back to their trans isomers. Irradiations of **1a−c** in oxygen-saturated chloroform-*d* yielded the corresponding cis isomers **2a−c** as the only products. The conversion of *E* to *Z* isomer for **1a** and **1b** decreased in oxygen-saturated chloroform-*d* in comparison to the case in argon-saturated chloroform-*d* but remained the same for **1c**. It should be noted that irradiation conditions for each compound in argon- and oxygen-chloroform-*d* were identical whereas the irradiations times were different for different compounds.

Because the product ratios are affected by O_2, we theorize there are two pathways for **1** to yield **2**, one, which is insensitive to oxygen, takes place on the singlet surface of **1**; the other pathway must be on the triplet surface of **1** as it is affected by oxygen.

Studies were performed with irradiation at different wavelengths, which led to different transient phenomena. The assignments made are shown in Scheme 3 to guide the reader through the results that support these assignments. We propose that the aryl ketone and the vinyl ketone chromophores in **1a**, **1b**, and **1c** are in cross-conjugation and can both absorb light, but that only the singlet excited aryl ketone, formed when the solution is irradiated at 308 nm, undergoes intersystem crossing to its triplet excited state (Scheme 3, horizontal pathway). The triplet ketone rearranges to form the triplet 1,2 biradical **3**. In

Scheme 3. Proposed Mechanism for the Cis−Trans Isomerization of 1a−c

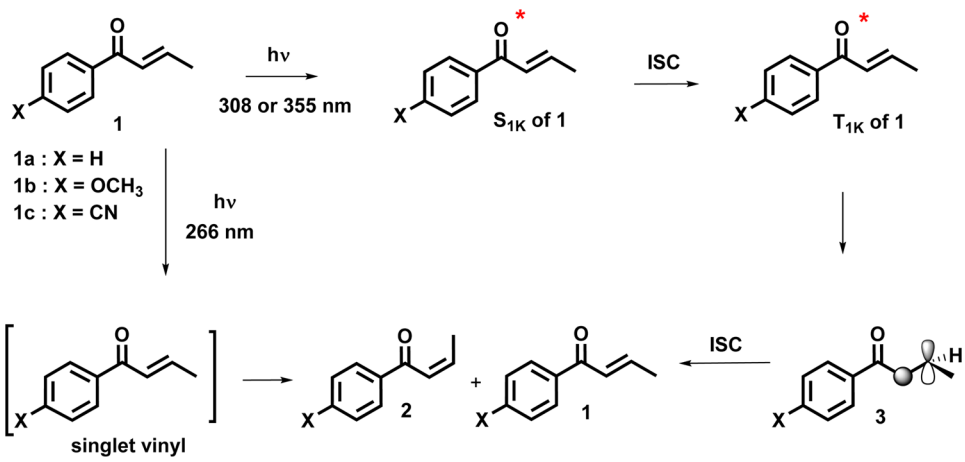

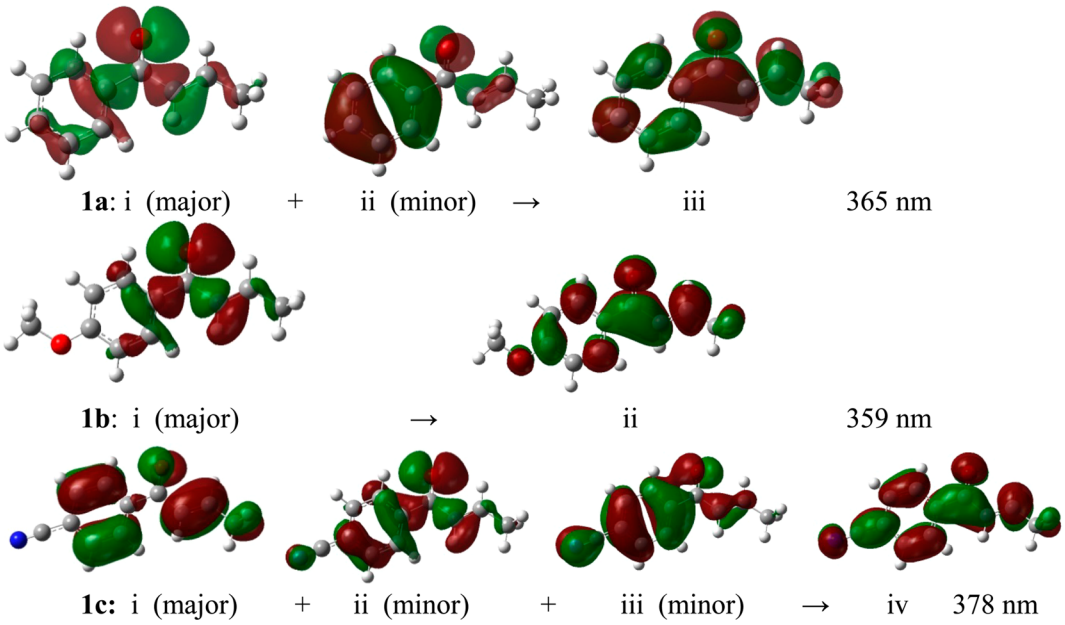

Figure 1. Calculated orbitals for the lowest energy electronic transfer in **1a**, **1b**, and **1c**.

contrast, the vinyl chromophore absorbs light at 266 nm to form its singlet excited state, which then decays to form **1** and **2**, directly on the singlet surface (Scheme 3, left vertical pathway).

2.2. Calculations. To better understand the isomerization of **1a**−**c**, we calculated stationary points on the triplet and singlet surfaces of **1a**−**c** using the Gaussian09 at the B3LYP level of theory and with the 6-31+G(d) basis set.[22−24]

We optimized ketones **1a**, **1b**, and **1c** and calculated the electronic transitions due to their ground state absorptions. These ketones have weak absorption bands at longer wavelengths that for **1a** and **1b** are due mainly to an electronic transition out of the lone pair on the oxygen atom into a π^*-orbital (Figure 1). In comparison, the major electronic transition for **1c** above 300 nm is an electronic transition out of a vinylic π-orbital into π^*-antibonding orbital. Thus, the calculations support that irradiation at longer wavelengths should mainly result in absorption of the ketone chromophores in **1a** and **1b** but not for **1c**.

We used TD-DFT calculations to locate the T_{1K} and T_{2K} of **1** and **2**, and the results are listed in Table 2. The calculations support that T_{1K} of **1a** and **1b** have similar energies, whereas the T_{1K} of **1c** is slightly lower in energy. The T_{2K} are just a few kcal/mol above the T_{1K} for **1** and **2**.

Table 2. Energies of the T_{1K} and T_{2K} of 1a, 1b, and 1c in kcal/mol

	phosphorescence[a]	optimization[b]	TD-DFT[c]	
	T_1	T_1	T_1	T_2
1a	73	62	67	71
1b	72	62	68	70
1c	71	60	64	69
2a		63	65	73
2b		63	68	73
2c		61	65	72

[a]Obtained from phosphorescence. [b]Obtained from optimization calculations. [c]Obtained from TD-DFT calculations.

We also optimized the structure of T_{1K} of **1** and **2**, which placed the energy of these triplet ketones considerably lower than the TD-DFT calculations. We have previously shown that DFT optimization of triplet ketones with (n,π^*) configuration underestimates their energy;[25−27] however, it is more likely that the energy difference is due to structural changes between the optimized structure of the T_{1K} of **1** and its S_0. Analysis of the calculated bond lengths in the T_{1K} of **1** and **2** shows that the C═O and the Cα—Cβ bonds are elongated in all of the ketones in comparison to the calculated bond lengths in the ground state (S_0, Figure 2). This indicates that the triplet ketones have a (n,π^*) configuration. Spin density calculations further support this notation as they place the unpaired electrons on the carbonyl oxygen atom and in the π^*-orbital on the vinyl bond (Scheme 4). The calculations suggest that T_{1K} of **1** and **2** are remarkably similar and are not affected by their *p*-phenyl substituent, thus demonstrating that these triplet ketones are best described as vinyl ketones rather than triplet acetophenones.

Optimization of triplet biradicals **3a**, **3b**, and **3c** show that they are located just a few kcal/mol below the T_{1K} of **1** and **2**. The calculated Cα−Cβ bonds in **3a**, **3b**, and **3c** are ∼1.5 Å, as they are single bonds, and the torsion angles between the CO−Cα−Cβ−Cγ are calculated to be ∼80° to avoid any overlap between the two radical centers. Spin density calculations place the unpaired electrons on the Cβ and Cα atoms, which have spin densities of −0.9 and −0.7, respectively (Scheme 5). The radical on the Cα atom is in conjugation with the carbonyl oxygen atom that has a spin density of −0.5, whereas the spin density is localized on the Cβ-atom. The calculations suggest that biradicals **3a**, **3b**, and **3c** are all remarkably similar and not affected by their *p*-substituent.

We calculated the transition state for the T_{1K} of **1** and **2** rearranging to form biradical **3**. These transitions states are located only a few kcal/mol above the T_{1K} of **1** and **2**, and in Figure 3, we have plotted stationary points on the triplet surface of **1** and **2**.

We calculated the rotational barrier for biradicals **3a**−**c** around their Cα−Cβ bond. As mentioned above, the biradicals

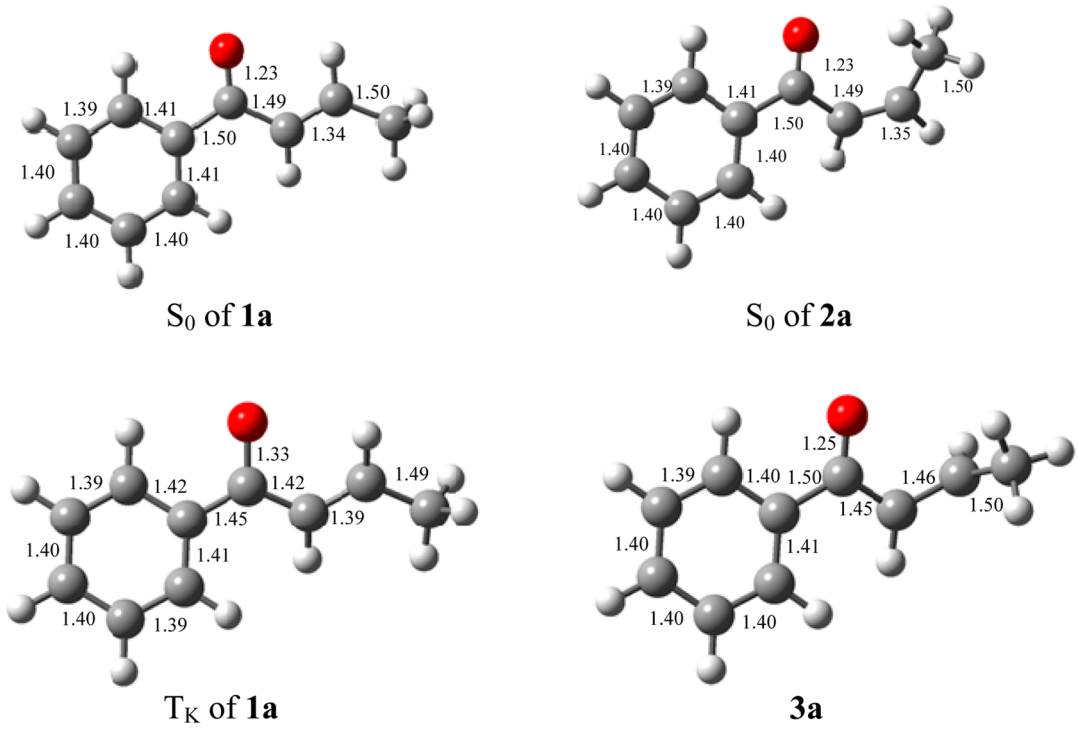

Figure 2. Optimized conformers of **1a**, the T_{1K} of **1a**, **2a**, and **3a**. The bond lengths are given in Å.

Scheme 4. Calculated Spin Densities for the T_{1K} of 1a, 1b, and 1c

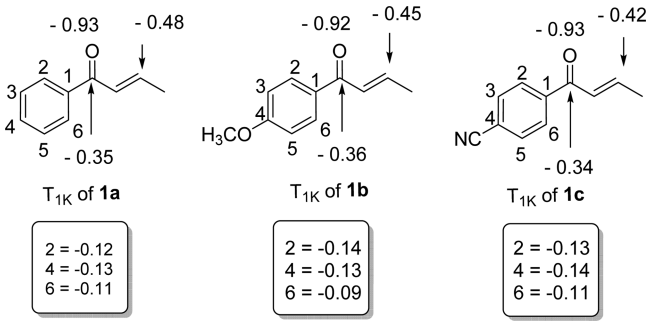

are the most stable as the two radical centers are almost perpendicular to each other or when the CO−Cα−Cβ−CH_3 torsion angle is 80°. The calculations suggest that further rotation around the Cα−Cβ bond brings the two radical centers closer together and destabilizes the biradicals. For example, for **3a**, the calculations imply that 6 kcal/mol (Figure 4) are required to reach the first rotational barrier where this torsion angle is 160° (Δ 80°). Interestingly, further rotation that makes the torsion angle closer to 180° yields the T_{1K} of **1a**. The calculated rotational barrier for **3a** to reach the T_{1K} of **2a** is slightly higher (8 kcal/mol), due to the steric demands of the methyl group. As expected, the calculated rotational barrier for the T_{1K} of **1a** around CO−Cα−Cβ−CH_3 yields the same rotation graph as for **3a**. From the graph, it can be seen that the rotational barriers for the T_{1K} of **1a** and **2a** forming **3a** are comparable to the transition state barrier for the T_{1K} of **1a** forming **3a**. We obtained similar results for **3b** and **3c**.

Finally, we optimized the peroxide radicals **4**, resulting from the addition of O_2 to biradicals **3a**, **3b**, and **3c** (Scheme 6). The calculations show that radicals **3a**, **3b**, and **3c** are expected to react similarly with O_2. The addition of O_2 to the radical centered on the Cβ atom results in resonance stabilized radical **4**. We cannot calculate the transition state barrier for O_2 adding to biradicals **3** due to spin restriction. In contrast, the calculated transition state barrier for peroxide radicals **4** extruding an O_2 molecule and forming **1** is only 3 kcal/mol above **4**.

2.3. Phosphorescence. We obtained phosphorescence spectra of **1a**, **1b**, and **1c** at 77 K in frozen ethanol matrices (Figure 5). The phosphorescence spectra of **1a**, **1b**, and **1c** show that they have emissions that do not have well-resolved emission bands as typically observed for ketones with (n,π*) configurations. Furthermore, the onset of the emission was

Scheme 5. Calculated Spin Densities for Triplet Biradicals 3a, 3b, and 3c

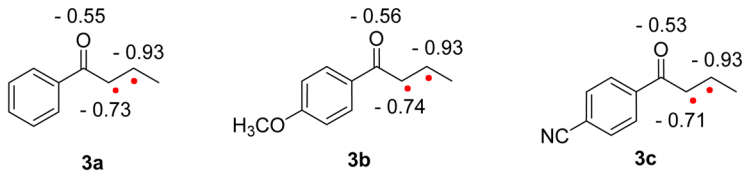

Dihedral angle	3a	3b	3c
H-Cα-Cβ-H	94.5°	96.1°	-93.7°
CO-Cα-Cβ-CH_3	79.9°	78.4°	-80.1°

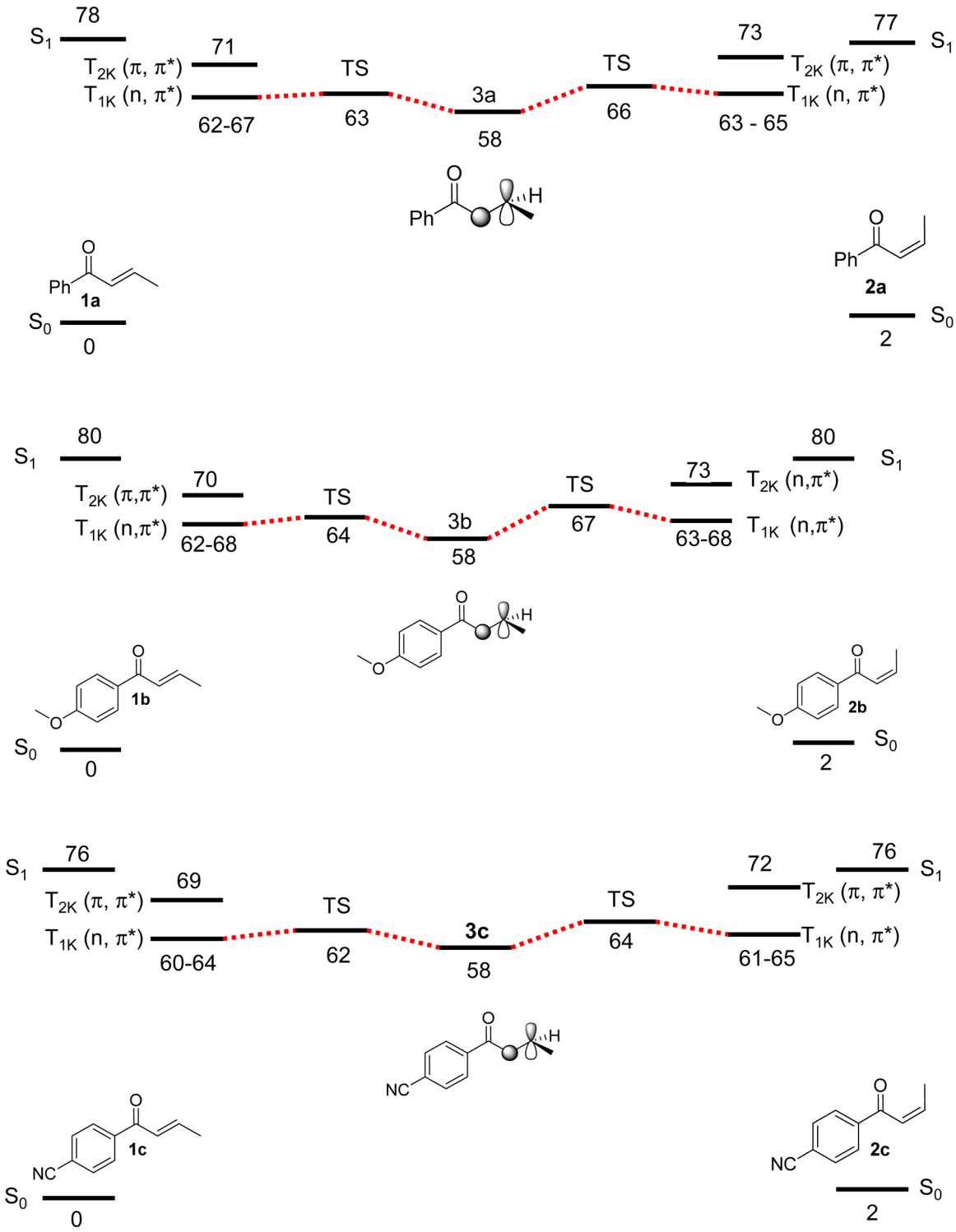

Figure 3. Calculated stationary points on the energy surface of **1a**, **1b**, and **1c**. TD-DFT calculations for **1b** place the triplet ketone with (π,π*) configuration below the (n,π*), whereas optimization places the (n,π*) ketone lower in energy.

used to estimate the (0,0) bands and is listed in Table 2. The energies from the emission spectra are considerably higher than energies obtained both from the optimization and from TD-DFT calculation of the T_{1K} of **1**. The calculated energies of the T_{2K} of **1** match better with the observed emission, and thus, we speculate that the emission is due to the T_{2K} of **1**. In addition, it should be noted that the relative intensitiy of phosphorescense for **1c** is considerably less than for **1a** and **1b**.

2.4. Laser Flash Photolysis. We performed laser flash photolysis to identify the excited state and intermediates formed upon irradiation of **1a**, **1b**, and **1c**. Laser flash photolysis (excimer laser, 308 nm, 17 ns)[28] of **1a** in argon-saturated acetonitrile produced a transient absorption with λ_{max} at ~360 nm and at ~460 nm (Figure 6). We assigned these absorption bands to the overlapping absorption of the T_{1K} of **1a** and **3a**, on the basis of their calculated spectra. The calculated TD-DFT absorption spectrum of the T_{1K} of **1a** in acetonitrile

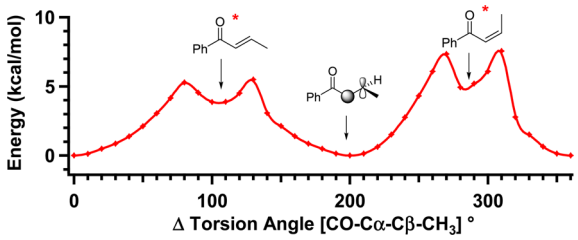

Figure 4. Calculated rotational barrier for **3a**.

has major electronic transitions at 469 (f = 0.1423), 327 (f = 0.0570), 326 (f = 0.0812), 316 (f = 0.1618), and 309 nm (f = 0.2403) (Figure 7), which fits well with the observed spectra. Furthermore, the calculated TD-DFT absorption spectrum of **3a** in acetonitrile is also similar to the observed spectrum as it has calculated electronic transitions at 469 (f = 0.0375), 437 (f = 0.0127), and 337 nm (f = 0.0452).

Kinetic analysis of the transient absorption further supported these assignments. The transient absorption at 420 nm in argon-saturated acetonitrile was fitted to a sum of two exponentials resulting in rate constants of 3.4×10^6 s^{-1} (τ = 308 ns) and 1.73×10^5 s^{-1} (τ = 5.7 μs, Figure 6). In O_2-saturated acetonitrile, the transient is formed faster than the time resolution of the instrument, and it decays with a rate constant of 1.16×10^7 s^{-1} (τ = 86 ns). As the decay in oxygen-saturated acetonitrile is a monoexponential decay, we conclude that oxygen shortens the lifetime of the T_{1K} of **1a** so we do not observe it; its lifetime must be less than the time resolution of the laser flash apparatus or 17 ns. Oxygen also reduces the lifetime of **3a** to 86 ns. As the concentration of O_2 in acetonitrile is 0.009 M,[29] we can determine that 1,2-biradical **3a** reacts with O_2 with a rate constant of 1.3×10^9 M^{-1} s^{-1}.

Analysis of the kinetics at 360 nm revealed similar results as obtained from the kinetics at 460 and 500 nm, but at 360 nm, there is a significant residual absorption due to the formation of **2a**, which makes it more complicated to obtain accurate lifetimes.

We used isoprene to quench the T_{1K} of **1a** (Figure 8). We measured the yield of absorbance versus isoprene concentration at 360 and 500 nm. This was required because it was complicated to directly measure the rate constant for the decay of **3a** as a function of isoprene concentration considering that the lifetime for ketone decay in the absence of quencher was already close to the time resolution of the system. The yields of the absorbance at 360 or 500 nm for the biradical decreased with increased isoprene concentration whereas the lifetime of the decay was not affected. Thus, isoprene quenches the T_{1K} of **1a** but not **3a**. Using the Stern−Volmer equation,

$$\frac{A_0}{A} = 1 + k_q \tau_0 [Q]$$

A_0 is the absorption of **3a** without any quencher, and A is the absorption of **3a** at various isoprene concentrations. k_q is the quenching rate constant of the triplet state; τ_0 is the lifetime of the T_1 of **1a** without any isoprene. [Q] is the concentration of the isoprene.

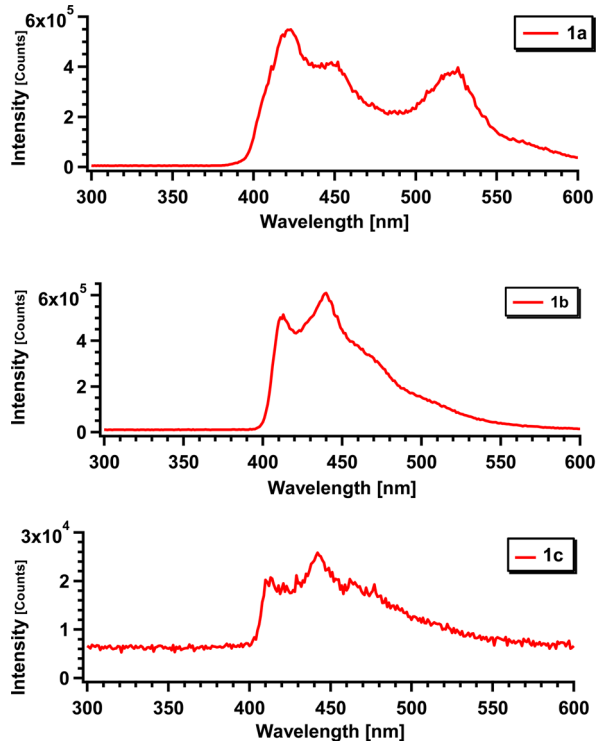

Figure 5. Phosphorescence of **1a**, **1b**, and **1c** in ethanol at 77 K with 300 nm excitation.

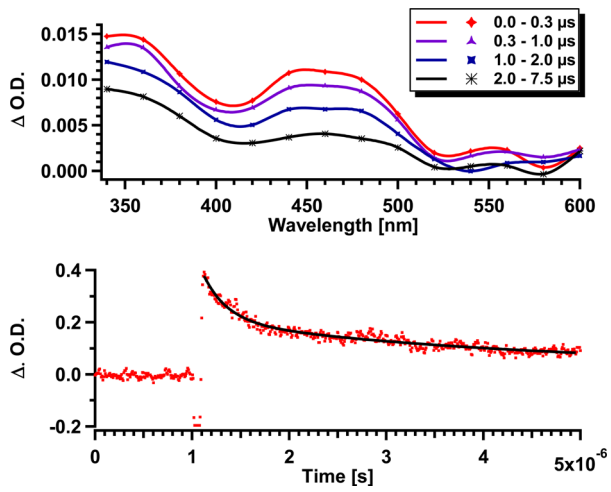

Figure 6. (a) Transient spectra obtained by laser flash photolysis of **1a** in argon-saturated acetonitrile with 308 nm laser excitation. (b) Kinetic trace obtained by laser flash photolysis of **1a** with 308 nm laser at 420 nm in argon-saturated acetonitrile.

Scheme 6

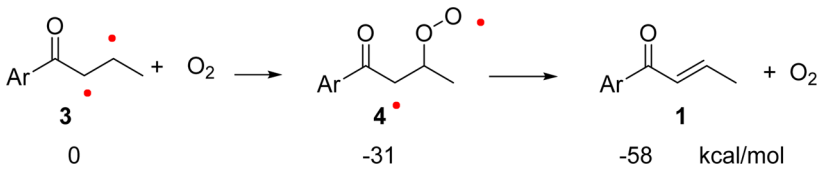

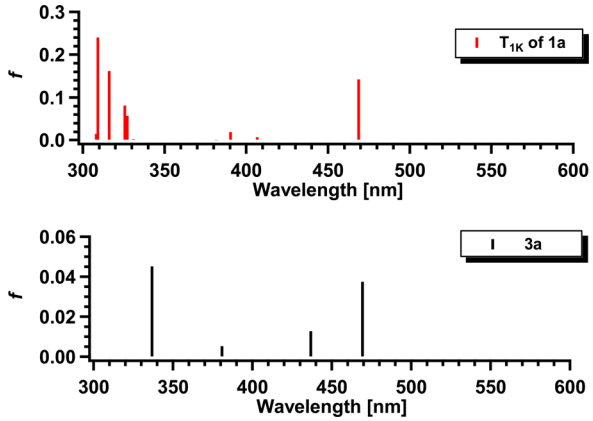

Figure 7. Calculated electronic transition for the T_{1K} of **1a** (top) and **3a** (bottom) in acetonitrile using the TD-DFT level of theory with the UB3LYP/6-31+G(d) basis set.

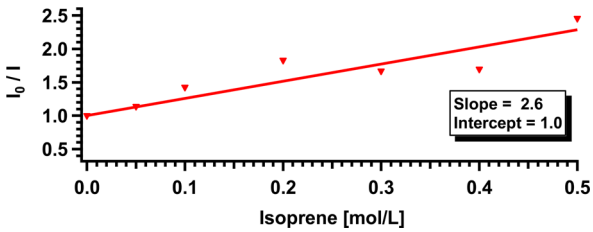

Figure 8. Stern–Volmer plot for quenching the T_{1K} of **1a** with isoprene at 360 nm.

We obtained a k_q value of 8×10^6 M^{-1} s^{-1} using the lifetime of the T_{1K} of **1a** as 308 ns at ambient temperature. The k_q value is considerably less than the rate constant for a diffusion controlled process, which was expected because the triplet energy of isoprene is 60 kcal/mol and thus similar to the triplet energy of the T_{1K} of **1a** that we estimated to be 62 kcal/mol.[30] Thus, the isoprene quenching demonstrated that the T_{1K} of **1a** is the precursor to **3a** and that the energy of the T_{1K} of **1a** is similar to the energy of the triplet excited isoprene.

To better evaluate the wavelength dependency of the photochemistry of **1a**, laser flash photolysis with a 355 nm Nd:YAG laser that has a 10 ns time resolution was performed.[31,32] The transient spectra obtained with 355 nm irradiation show a negative absorption at approximately 350 nm due to the bleaching of **1a**, as a higher concentration of the starting material is needed in this case compared to the experiments conducted with 308 nm irradiation to ensure that for the excitation at 355 nm the absorption was sufficiently high for the detection of transients (Figure 9). In addition, the transient spectra formed from 355 nm irradiation were obtained using a flow cell and, thus, had less residual absorption due to product formation than observed in the transient spectra obtained with the 308 nm irradiation. Therefore, excitation at 355 nm resulted in spectra with a somewhat broader appearance.

The kinetic analysis obtained with 355 nm excitation showed a decay that can be fitted to a sum of two exponentials with lifetimes of 295 ns and 6 μs, which matches, within experimental errors, the lifetimes of the T_{1K} of **1** and **3a** obtained from 308 nm irradiation. In oxygen-saturated acetonitrile, the faster component, T_{1K} of **1a** is fully quenched and the absorption of **3a** decays with a rate constant of 7.9×10^6 s^{-1} (τ = 126 ns) or the rate constant for **3a** reacting with O_2

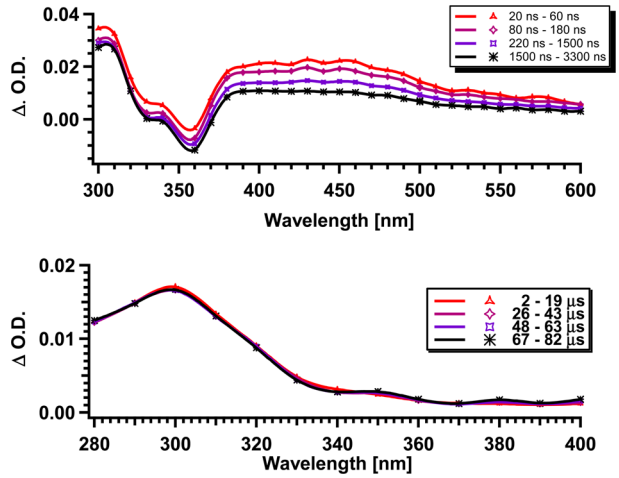

Figure 9. Laser flash photolysis of **1a** in nitrogen-saturated acetonitrile with (a) λ = 355 nm irradiation and (b) λ = 266 nm irradiation.

at 0.009 M concentration is 8.8×10^8 M^{-1} s^{-1},[29] which is in agreement, within experimental error, with the rate constant determined from the 308 nm irradiation.

We also performed laser flash photolysis of **1a** using 266 nm irradiation (Nd:YAG laser, 266 nm, 10 ns)[31,32] in nitrogen-saturated acetonitrile that produced a broad absorption with a λ_{max} at ~300 nm (Figure 9). This absorption remained constant at shorter time scales but decayed with a rate constant of ca. 0.38 s^{-1} (τ = 2.6 s) at longer time scales. We assigned this absorption to formation of **2a** and the decay to the diffusion of **2a** out of the detection pathway.[31]

Laser flash photolysis (Excimer laser, 308 nm, 17 ns) of **1b** in argon-saturated acetonitrile produced a broad transient absorption with λ_{max} at ~360 nm that trails out to 600 nm (Figure 10a). We assigned this absorption to the overlapping

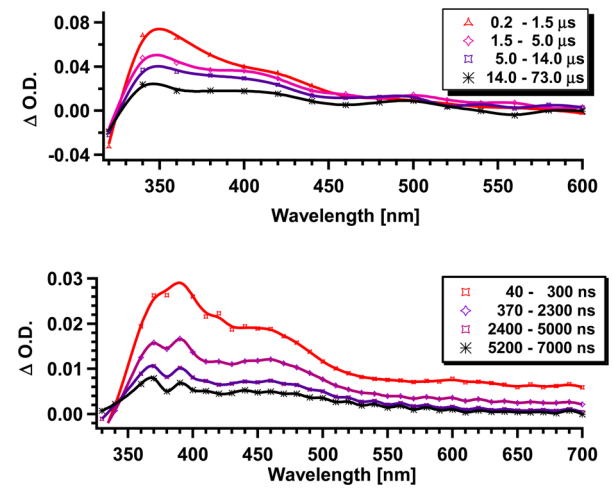

Figure 10. Transient spectra obtained by laser flash photolysis of **1b**: (a) argon-saturated acetonitrile with 308 nm irradiation and (b) nitrogen-saturated acetonitrile with 355 nm irradiation.

absorption of the T_{1K} of **1b** and the **3b** on the basis of the TD-DFT calculations. The calculated TD-DFT absorption spectrum of the T_{1K} of **1b** in acetonitrile has major electronic transitions at 498 (f = 0.034), 477 (f = 0.1351), 335 (f = 0.1856), and 327 nm (f = 0.3323), which fits well with the observed spectrum (Figure 11). In comparison, the calculated

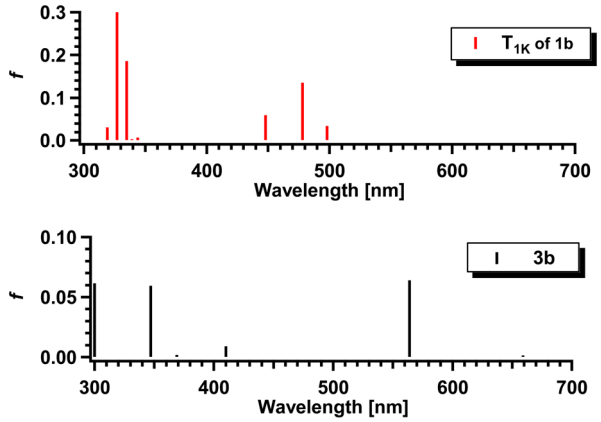

Figure 11. Calculated electronic transition of the T_{1K} of **1b** (top) and **3b** (bottom) in acetonitrile using the TD-DFT level of theory with the UB3LYP/6-31+G(d) basis set.

TD-DFT absorption spectrum of **3b** in acetonitrile has major electronic transitions at 564 (f = 0.0640), 347 (f = 0.0594), and 300 nm (f = 0.0615). The calculations demonstrate that **3b** has less intense electronic transitions that are buried under the absorption for the T_{1K} of **1b** at shorter wavelengths, but at longer wavelengths **3b** has more significant absorption, which fits nicely with the observed experimental spectra. Laser flash photolysis (Nd:YAG laser, 355 nm, 10 ns) of **1b** in argon-saturated acetonitrile allowed us to measure the absorption out to 700 nm, which showed a broad transient absorption with a λ_{max} at ~360 nm that trailed out to 700 nm (Figure 10b).

Kinetic analyses of the transient absorption obtained with 308 and 355 nm irradiation were the same, within experimental error, and further supported the assignment of the transient absorption to the T_{1K} of **1b** and **3b**. The transient absorption at 400 nm can be fitted as a sum of two exponentials, yielding rate constants of 4.6×10^6 s^{-1} (τ = 215 ns) and 3.2×10^5 s^{-1} (τ = 3.1 μs) (Figure 12). We assigned the shorter decay to the T_{1K} of **1b** and the longer one to **3b**. The absorption at 330 nm grew in with a rate constant of 2.5×10^5 s^{-1} (τ = 3.9 μs), which is consistent with **2b** being formed with the same rate constant as observed for the decay of **3b**. In oxygen-saturated acetonitrile, a monoexponential decay was observed with a decay rate

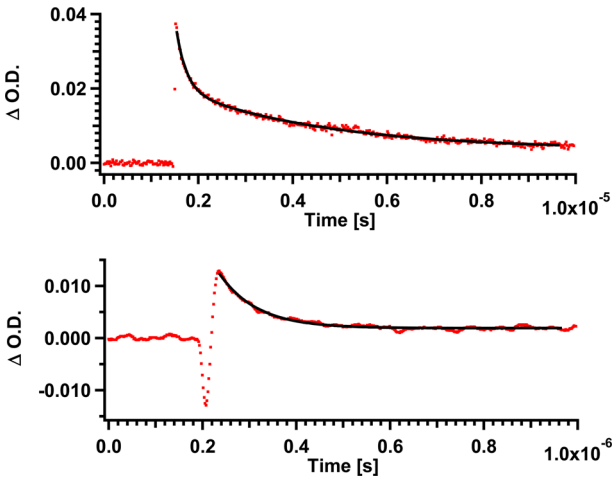

Figure 12. Kinetic traces obtained at (a) 400 nm in nitrogen-saturated acetonitrile and (b) 440 nm in oxygen-saturated acetonitrile with 355 nm irradiation of **1b**.

constant of 1.4×10^7 s^{-1} (τ = 74 ns); thus, we conclude that oxygen shortens the lifetime of the T_{1K} of **1b** so we do not observe it, its lifetime must be less than the time resolution of the laser flash apparatus or 17 ns. It also reduces the lifetime of **3b** to 74 ns. As the concentration of O_2 in acetonitrile is 0.009 M,[29] the rate constant for **3b** reacting with oxygen was estimated to be 1.5×10^9 M^{-1} s^{-1}.

Laser flash photolysis (excimer laser, 308 nm, 17 ns) of **1c** in argon-saturated acetonitrile produced a transient absorption with a λ_{max} at ~360 nm (Figure 13). The intensity of the band

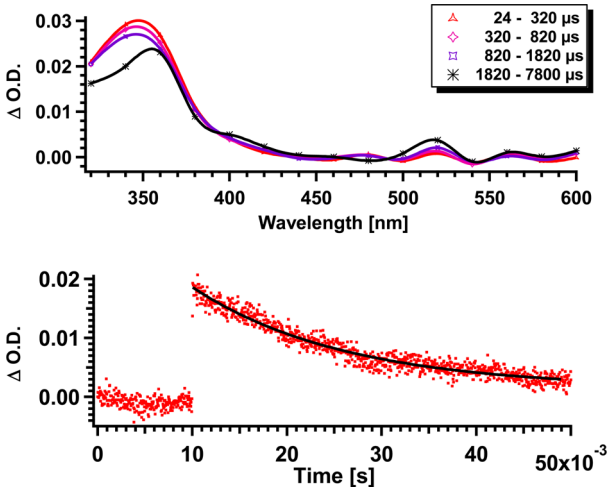

Figure 13. (a) Laser flash photolysis of **1c** in argon-saturated acetonitrile. (b) Kinetics obtained by laser flash photolysis of **1c** in argon-saturated acetonitrile at 360 nm with 308 nm irradiation.

at 360 nm remains constant on shorter time scales, but on millisecond time scales, we observe some decay of the signal. The calculated spectra for the T_{1K} of **1c** (Figure 14) fit with the observed spectra, but it is not reasonable to expect a triplet ketone to have lifetime on the millisecond time scale. The calculated absorption for **3c** does not match with the observed spectra, and therefore, we assign the absorption at 360 nm to the formation of photoproduct **2c** and the decay to diffusion of the transient out of the detection volume.

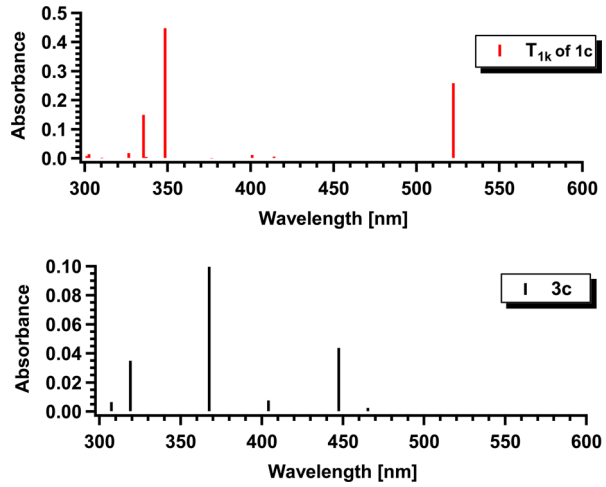

Figure 14. Calculated UV of the T_{1K} of **1c** (top) and the T_{BR} of **1c** (bottom) in acetonitrile using TD-DFT level of theory with the UB3LYP/6-31+G(d) basis set.

Kinetic analysis of the transient absorption further supports this assignment. The transient absorption at 360 nm does not decay on shorter time scales but does on millisecond time scales with a rate constant of <62 s^{-1} (τ >16 ms, Figure 13b), which must be due to **2c** diffusing out of the monitoring path.

Thus, laser flash photolysis confirms that irradiation of **1a** and **1b** results in formation of their triplet ketones, which decay to form biradicals **3a** and **3b**, respectively. Biradicals **3a** and **3b** have a lifetime of a few microseconds and react with molecular oxygen with rate constants on the order of 0.88 and 1.5×10^9 M^{-1} s^{-1}. In comparison, laser flash photolysis of **1c** did not yield the T_{1K} of **1c** or biradical **3c**, either because the T_{1K} of **1c** and biradical **1c** are too short-lived or because **1c** reacts only on the singlet excited state surface to yield **2c**.

2.5. Time-Resolved Infrared (TRIR) Spectroscopy. To verify that the irradiation of **1a** with 266 nm irradiation yields **2a** in the singlet surface, we performed time-resolved infrared (TRIR) spectroscopy of **1a** in cyclohexane. TRIR difference spectra from 1750 to 1500 cm^{-1} were monitored over the first 45 μs following 266 nm laser photolysis (Figure 15).

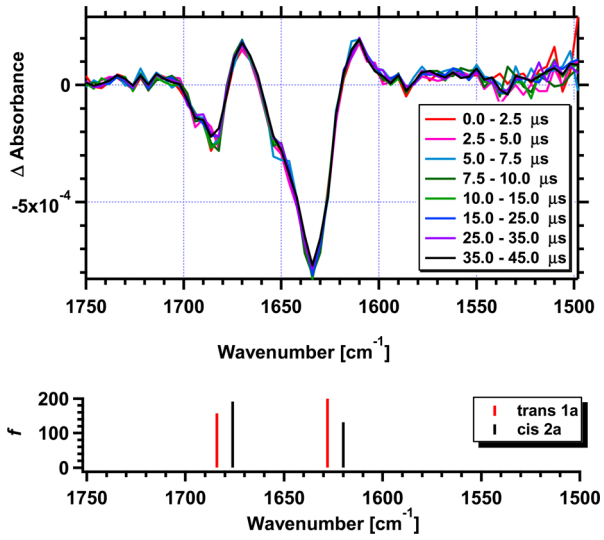

Figure 15. TRIR difference spectra averaged over the time scales indicated following 266 nm laser photolysis of **1a** in (a) argon-saturated cyclohexane at room temperature. (b) Calculated C═O and C═C vibrations of **1a** and **2a** using TD-DFT level of theory with B3LYP/6-31+G(d) basis set (scaling factor = 0.9613[33]).

Immediately after the laser pulse, two negative bands were observed at 1685 and 1635 cm^{-1}, which are due to the depleted C═O and C═C stretches of **1a**. Concurrent to the depletion of the bands at 1685 and 1635 cm^{-1}, two new bands were formed at 1670 and 1610 cm^{-1}, which are assigned to the C═O and C═C stretches of **2a**. These assignments are based on the observed and calculated IR spectrum of **2a** (Figure 15b). Analysis of the kinetics showed that on microsecond time scales the bands due to depletion of **1a** and formation of **2a** did not change over time. Furthermore, these bands were not affected by molecular oxygen. Thus, the 266 nm irradiation of **1a** results in cis−trans isomerization on its singlet excited state surface.

2.6. Matrix Isolation. We studied the photochemistry of **1a**, **1b**, and **1c** in argon matrices at 14 K to confirm that they undergo cis−trans isomerization at cryogenic temperatures. Upon irradiation of **1a**, significant new bands were formed at 1678, 1661, 1609, 1558, 1453, 1229, 1014, 837, 737, and 730 cm^{-1} concurrently with the decrease of the bands at 1688, 1668, 1654, 1612, 1562, 1447, 1299, 1219, 1222, 1025, 831, 757, and 720 cm^{-1} (Figure 16). We assigned all the new bands

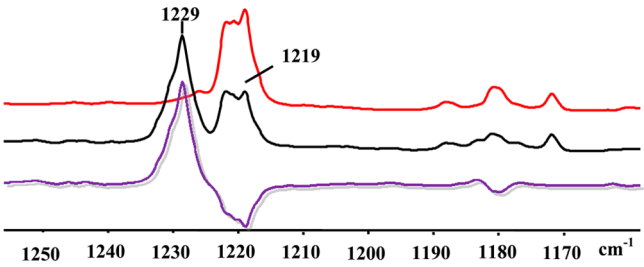

Figure 16. IR spectra of **1a** (a) before irradiation (red) and (b) after irradiation (black) and (c) the difference spectrum (purple).

to **2a**, on the basis of comparison to its reported IR and calculated spectra. In Table 3 are listed all the IR bands that were formed or depleted upon irradiation, along with their assignments based on calculations.

Table 3. IR Bands Formed or Reduced upon Irradiation of 1a in Argon Matrices and Comparison of the Observed and Calculated IR Bands of 1a and 2a

experimental IR bands cm^{-1}			calculated IR bands cm^{-1}		
formed	reduced	Δ	**2a**	**1a**	Δ
1678	1688	−10	1727 (190)	1736 (156)	−11
1661	1668	−7	1670 (131)	1678 (199)	−8
1609	1612	−3	1628 (11)	1627 (13)	+1
1558	1562	−4	1503 (23)	1506 (47)	−3
1453	1447	+6	1495 (46)	1498 (9)	−3
	1299		1293 (2)	1331 (82)	
1229	1219	+10	1249 (233)	1243 (162)	+6
1014	1025	−11	1031 (49)	1046 (24)	−15
837	831	+6	853 (10)	843 (11)	+10
737	757	−20	751 (90)	775 (30)	−24
730	720	+10	699 (17)	685 (9)	+14

Irradiation of **1b** in argon matrices at 14 K led to the formation of new absorption bands at 1676, 1605, 1538, 1268, 1242, 1233, 1171, 1088, 795, and 787 cm^{-1} concurrently with the decrease of the bands at 1681, 1608, 1539, 1299, 1260, 1225, 1221, 1173, 812, and 801 cm^{-1}. As before, we assigned the new bands to **2b** on the basis of its reported spectrum and calculations (Figure 17, Table 4).

Upon irradiation of **1c**, new bands were formed at 2240, 1681, 1624, 1370, 1368, 1223, 1026, 1015, 909, 789, 787, 768, 716, and 552 cm^{-1} concurrently as the intensity of the following bands decreased 2237, 1688, 1671, 1634, 1380, 1378, 1301, 1220, 1217, 1041, 1020, 918, 811, 809, 760, and 542 cm^{-1}. As before, we assign the new bands to **2c** on the basis of its IR spectrum and calculations (Figure 18, Table 5).

The matrix isolation experiments show that **1a**, **1b**, and **1c** undergo efficient cis−trans isomerization at cryogenic temperatures. However, we cannot identify whether these isomerizations take place through the singlet or triplet surfaces of **1a**−**c**.

3. DISCUSSION

The photochemistry of **1a** and **1b** is wavelength dependent, where irradiation at longer wavelengths allows for selective

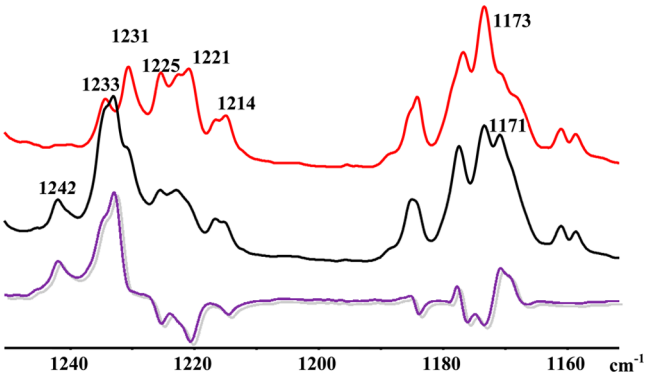

Figure 17. Matrix IR spectra of **1b** before irradiation (red) and after irradiation (black) and the difference spectrum (purple).

Table 4. IR Bands Formed or Reduced upon Irradiation of 1b in Argon Matrices and Comparison of the Observed and Calculated IR Bands of 1b and 2b

experimental IR bands cm^{-1}			calculated IR bands cm^{-1}		
formed	reduced	Δ	**2b**	**1b**	Δ
1676	1681	−5	1723 (182)	1733 (158)	−10
1605	1608	−3	1649 (262)	1653 (263)	−4
1538	1539	−1	1504 (25)	1507 (53)	−3
	1299			1327 (32)	--
1268	1260	+8	1302 (205)	1296 (271)	+6
1233	1225/1221	+8/+12	1259 (351)	1248 (250)	+11
1242			1293 (16)		
1171	1173	−2	1201 (255)	1210 (143)	−9
1088			1043 (57)	1050 (36)	−7
787	812	−25	810 (59)	840 (32)	−30
795	801	−6	801 (22)	794 (1)	+7

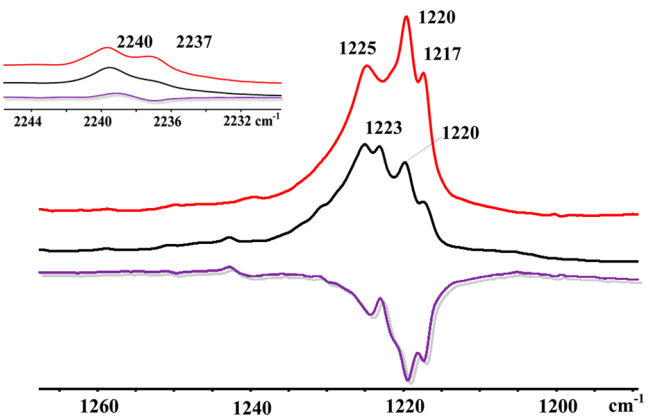

Figure 18. Matrix IR of **1c** before irradiation (red) and after irradiation (black) and the difference spectrum (purple).

irradiation into the ketone chromophore, as supported by the TD-DFT calculations.

The singlet excited ketones intersystem cross to their triplet excited states, which rearrange to yield triplet 1,2-biradicals **3a** and **3b**. In contrast, irradiation at shorter wavelengths leads to excitation into the vinyl excited state that results in cis−trans isomerization on the singlet surface (Scheme 3). It was not possible to selectively irradiate into the ketone chromophore of **1c**, and thus, its excited state only undergoes isomerization on its singlet surface. The TD-DFT calculations support that selective excitation into the ketone chromophore **1c** is not possible. Furthermore, as the calculated properties of the T_{1K} of **1c** and **2c** are similar to those of the T_{1K} of **1a** and **1b** and biradicals **3a** and **3b**, it is unlikely that the T_{1K} of **1c** and **2c** are too short-lived to be observed. Further support that **1c** does not undergo triplet reactivity comes from the phosphorescence studies that show that the emission relative intensity for **1c** is significantly lower than for **1a** and **1b**.

Table 5. IR Bands Formed or Reduced upon Irradiation of 1c in Argon Matrices and Comparison of the Observed and Calculated IR Bands of 1c and 2c

experimental IR bands cm^{-1}			calculated IR bands cm^{-1}		
formed	reduced	Δ	**2c**	**1c**	Δ
2240	2237	+3	2336 (36)	2336 (36)	0
1681	1688	−7	1730 (194)	1737 (165)	−7
1624	1634	−10	1670 (165)	1678 (235)	−8
1370	1380	−10	1423 (18)	1434 (2)	−11
1368	1378	−10			
	1301		1294 (2)	1331 (75)	−37
1223	1220/1217	+3/+6	1245 (244)	1243 (171)	+2
1026	1041	−15	1047 (20)	1062 (29)	−15
1015	1020	−5	1030 (47)	1035 (13)	−5
909	918	−9	925 (57)	934 (81)	−9
789	811	−22	808 (60)	831 (38)	−23
787	809	−22			
768	760	+8	784 (16)	774 (14)	+10
716			731 (13)	748 (2)	−17
552	542	+10	564 (15)	559 (10)	+5

Biradicals **3a** and **3b** reacted with molecular O_2 with rate constants of $(0.88–1.3) \times 10^9$ and 1.5×10^9 M^{-1} s^{-1}, respectively, which is somewhat lower than the quenching of their triplet ketone precursors with O_2. Spin restriction prevents us from calculating the transition state for O_2 adding to biradicals **3a** and **3b** (Scheme 7) to form **4**. However, it can be theorized that peroxy radical **4** extrudes molecular O_2 to form **1a** and **1b**, as the calculated transition state barrier for extruding an O_2 molecule is only a few kcal/mol above the peroxide biradical. It is also possible that molecular O_2 quenches biradicals **3a** and **3b** by energy transfer similarly to how O_2 quenches the T_{1K} of **1a** and **1b**. Thus, adding O_2 to triplet 1,2-biradicals is not expected to yield any new products but rather to regenerate **1a** and **1b** or **2a** and **2b**.

Scheme 7

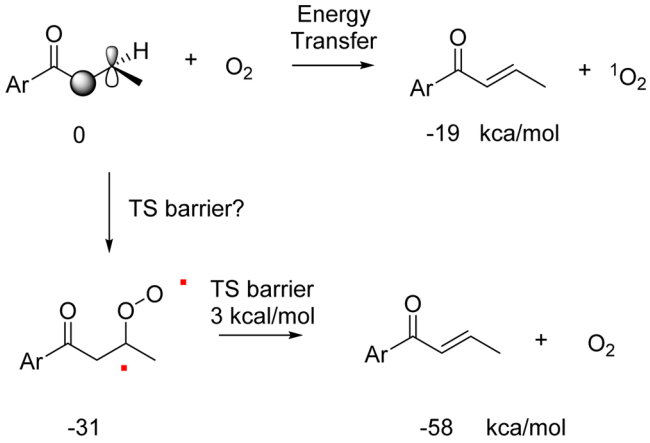

Phosphorescence emission of **1** results in an emission that has considerably higher energy than the one obtained from calculations, and thus, it seems plausible that at lower temperatures we are observing emission from the T_{2K} of **1** rather than the T_{1K} of **1**. It should be highlighted that the quenching studies with isoprene, however, support that the precursor to **3a** is the T_{1K} of **1** that has triplet energy similar to that for isoprene.

The lifetimes of **3a** and **3b** are similar to the lifetimes that Garcia-Exposito et al. reported for triplet biradicals from 2-pentenoate esters that have lifetimes between 1 and 16 μs.[19] As mentioned earlier, the authors theorized that the lifetime of their biradicals was limited due to intersystem crossing, which depends on the energy gap between the singlet and the triplet surface and is enhanced by spin−orbit coupling. Furthermore, the authors concluded that the largest spin−orbit coupling was obtained when the torsional angle between the two radicals is approximately 45°, and therefore, intersystem crossing should take place as the biradicals rotate into this conformer. The calculated energy between the ground state of **1** and triplet biradicals **3** is similar to the 2-pentenoate system, and thus, these biradicals must decay by a similar mechanism.

4. CONCLUSION

Thus, we have shown that intramolecular sensitization can be used to selectively form triplet 1,2-biradicals from simple vinylalkenes. The biradicals have lifetimes of a few microseconds in acetonitrile and are efficiently quenched with molecular O_2. As cis−trans isomerization has potential use in several applications, it is important to evaluate how spin delocalization and rotational barriers affect the lifetimes of the 1,2-biradicals and, thus, the cis−trans isomerization.

5. EXPERIMENTAL SECTION

5.1. Calculations. All geometries were optimized at B3LYP level of theory and with 6-31G+(d) basis set as implemented in the Gaussian09 programs.[22−24] All transition states were confirmed to have one imaginary vibrational frequency. Intrinsic reaction coordinates calculations were used to verify that the located transition states corresponded to the attributed reactant and product.[34,35] The absorption spectra were calculated using time-dependent density functional theory (TD-DFT).[36−40] The effect of solvation was calculated using the self-consistent reaction field (SCRF) method with the integral equation formalism polarization continuum model (IEFPCM) with acetonitrile, methanol, and dichloromethane as solvents.[41−45]

5.2. Laser Flash Photolysis. Laser flash photolysis was performed with an excimer laser (308 nm, 17 ns)[28] or Nd:YAG laser (266 or 355 nm, 10 ns).[31,32] A stock solution of **1a−c** in acetonitrile was prepared with spectroscopic grade acetonitrile, such that the solutions had absorption between 0.3 and 0.6 at the excitation wavelength. Typically, ∼1 mL of the stock solution was placed in a 10 mm × 10 mm wide, 48 mm long quartz cuvette and was purged with argon for 5 min or oxygen for 5 min. The rate constants were obtained by fitting an average of three to five kinetic traces.

For the experiments using the Nd:YAG laser for excitation, a home-built flow cell was employed where the irradiation occurred in a cell with a 7 mm × 7 mm cross section. A syringe pump was used to pump the solution through the cell and a reservoir, which was continuously purged with nitrogen or oxygen, contained the solution used. The flow rate was increased until the interference from product formation disappeared; i.e., the shape of the decay and the final offset were the same when the flow rate was increased further.

5.3. Time-Resolved IR Methods. TRIR experiments were conducted (with 16 cm^{-1} spectral resolution) following the method of Hamaguchi and co-workers,[46,47] as has been described previously.[48] Briefly, the broadband output of a $MoSi_2$ IR source (JASCO) is crossed with excitation pulses from a Continuum Minilite II Nd:YAG laser (266 nm, 5 ns, 2 mJ) operating at 15 Hz. Changes in IR intensity are monitored using an AC-coupled mercury/cadmium/tellurium (MCT) photovoltaic IR detector (Kolmar Technologies, KMPV11-J1/AC), amplified, digitized with a Tektronix TDS520A oscilloscope, and collected for data processing. The experiment is conducted in dispersive mode with a JASCO TRIR 1000 spectrometer. Sample preparations were performed as described the literature.[48]

5.4. Matrix Isolation. Matrix isolation studies were performed using conventional equipment.[49] Matrix isolation experiments were conducted using standard high vacuum techniques. Argon gas flowed over the solid sample, entraining the vapor above the solid, and was deposited onto a CsI cold window cooled to 14 K by a CTi closed cycle refrigerator. Infrared spectra were recorded at 1 cm^{-1} resolution by a PerkinElmer Spectrum One FTIR during and after matrix deposition. The matrix was then irradiated by the Pyrex-filtered light of a medium pressure mercury arc lamp after which additional spectra were recorded.

5.5. Phosphorescence. Ethanol solutions of **1a** (1 mM), **1b** (0.02 M), and **1c** (0.02 M)) were prepared, and their phosphorescence spectra were obtained at 77 K (Horiba Instruments Inc., Edison, NJ, USA; Horiba Jobin-Yvon fluorolog with 5 nm as the emission monochromator bandwidth). The solutions were irradiated at 300 and 260 nm and the emission spectra recorded between 300 and 800 nm.

5.6. Preparations of Starting Materials. *5.6.1. Synthesis of **1a**. 5.6.1.1. 1-Phenylbut-3-en-1-ol.* 1-Phenylbut-3-en-1-ol was synthesized following a modified procedures of El Bouakher et al.[50] and Bates and Sridhar.[51] Benzaldehyde (10.6 g, 0.10 mol) was dissolved in DMF (25 mL) and to the resulting solution was added allyl bromide (14.4 g, 0.12 mol, 1.2 equiv) and $SnCl_2$ (40.0 g, 0.20 mol, 2 equiv). NaI (20.0 g, 0.13 mol, 1.3 equiv) was added one spatula at a time slowly over a period of 10 min. Additional DMF (75 mL) was added to the mixture, and it was stirred overnight (20 h). NH_4F (30.0 g, 1.10 mol, 11 equiv) was dissolved in H_2O (100 mL), and the solution was added to the reaction mixture to quench the reaction. Diethyl ether (100 mL) was added, and the mixture stirred for further 30 min. The ether layer was extracted and washed twice with water (100 mL) and dried over anhydrous $MgSO_4$. The ether layer was evaporated under reduced pressure to give crude 1-phenylbut-3-en-1-ol (14.3 g, 0.10 mol, 96.8% yield). ^{1}H NMR, ^{13}C NMR, and IR spectra match the ones reported in the literature.[52] ^{1}H NMR ($CDCl_3$, 400 MHz): δ 2.4 (t, J = 6.8 Hz, 2H, $-CH_2-$), 2.7 (br s, 1H, −OH), 4.6 (t, J = 6.8 Hz, 1H, −CH), 5.08−5.13 (m, 2H, $=CH_2$), 5.7−5.8 (m, 1H, =CH), 7.2−7.3 (m, 5H, Ph-H) ppm. IR (neat): 3371 (br, OH), 3076, 3030, 3007, 2979, 2933, 2906, 1950, 1875, 1811, 1641, 1603, 1494, 1454, 1433, 1416, 1358, 1316, 1198, 1115, 1077, 1048, 1000, 916, 871, 830, 758, 700, 643, 609, 538 cm^{-1}.

5.6.1.2. Synthesis of 1-Phenylbut-3-en-1-one. The synthesis of 1-phenylbut-3-en-1-one was carried out by following a procedure reported by Hathaway and Paquette with some minor modifications.[53] CrO_3 (4.0 g, 0.04 mol) was dissolved in H_2SO_4 (4 mL, 12 N) acid to form a slurry, and water (12 mL) was added to make the Jones reagent (H_2CrO_4). The crude 1-phenylbut-3-en-1-ol (14.3 g, 0.10 mol) was dissolved in cold acetone (100 mL) and then 0.8−1.0 mL of H_2CrO_4 was added to the 1-phenylbut-3-en-1-ol while stirring at 0 °C until the green color of the reaction mixture changed to orange. The solution was filtered, the solvent was removed under reduced pressure, and the residue was dissolved in diethyl ether (100 mL) and washed with water (100 mL), saturated $NaHCO_3$ (100 mL), and brine (100 mL). The ether layer was dried over anhydrous $MgSO_4$, and the solvent was removed under reduced pressure to give 1-phenylbut-3-en-1-one (11.1 g, 0.08 mol, 78.5% yield). ^{1}H NMR, ^{13}C NMR, and IR spectra match those reported.[54] ^{1}H NMR ($CDCl_3$, 400 MHz): δ 3.7 (d, J = 6.8 Hz, 2H, $-CH_2-$), 5.16−5.21 (m, 2H $=CH_2$), 6.0−6.1 (m, 1H, =CH), 7.4 (t, J = 7.6 Hz, 2H, Ph-H), 7.5 (t, J = 7.6, Hz, 1H, Ph-H), 7.9 (d, J = 7.2 Hz, 2H, Ph-H) ppm. IR (neat): 3081, 1683 (s, C=O), 1645, 1598, 1581, 1449, 1425, 1395, 1334, 1276, 1210, 1180, 1004, 922, 755, 690, 617, 593 cm^{-1}.

*5.6.1.3. Synthesis of 1-Phenylbut-2-en-1-one (**1a**).* 1-Phenylbut-3-en-1-one (11.1 g, 0.08 mol) from the reaction above was dissolved in methanol (100 mL), and triethylamine (3−4 drops) was added. The reaction mixture was stirred overnight (20 h), the solvent was removed under reduced pressure, and the residue was extracted with diethyl ether (100 mL) and washed with water (100 mL). The ether layer was dried over anhydrous $MgSO_4$, the solvent removed under reduced pressure, and the residue was purified on a silica column eluted with ethyl acetate/hexane (1:4) to yield **1a** (1-phenylbut-2-en-1-one) (4.5 g, 0.03 mol, 31% yield). The ^{1}H NMR, ^{13}C NMR, and IR spectra of **1a** match those reported.[55] ^{1}H NMR ($CDCl_3$, 400 MHz): δ 2.0 (d, J = 6.8 Hz, 3H, $-CH_3$), 6.9 (d, J = 15.2 Hz, 1H, =CH), 7.0−7.1 (m, 1H, =CH), 7.4 (t, J = 7.4 Hz, 2H, Ph-H), 7.5 (t, J = 7.4 Hz, 1H, Ph-H), 7.9 (d, J = 8 Hz, 2H, Ph-H) ppm. ^{13}C NMR ($CDCl_3$, 100 MHz): δ 18.6, 127.6, 128.5, 132.6, 137.9, 145.0, 190. Eight ppm. IR (neat): 3058, 2912, 1702, 1673 (s, C=O), 1598, 1579, 1448, 1332, 1297, 1220, 1179, 1038, 1024, 965, 918, 830, 759, 693, 664 cm^{-1}. GC/MS (EI): m/z: 146 (M^+), 131, 117, 105 (100%), 77, 69.

*5.6.2. Preparation of **1b**. 5.6.2.1. Synthesis of 1-(4-Methoxyphenyl)-but-3-en-1-ol.* Using the procedure described above, anisaldehyde (13.5 g, 0.10 mol) and allyl bromide (14.4 g, 0.12 mol, 1.2 equiv) resulted in 1-(4-methoxyphenyl)but-3-en-1-ol (15.6 g, 0.09 mol) in 88% yield. ^{1}H NMR, ^{13}C NMR, and IR spectra obtained of **1a** match those reported.[56] ^{1}H NMR ($CDCl_3$, 400 MHz): δ 2.0 (d, J = 2.8 Hz, 1H, −OH), 2.5 (t, J = 6.8 Hz, 2H, $-CH_2$), 3.8 (s, 3H, $-OCHH_3$), 4.7 (dt, J = 6.4 Hz, J = 2.4 Hz, 1H, −CH), 5.11−5.12 (m, 2H, $=CH_2$), 5.7−5.8 (m, 1H, =CH), 6.9 (d, J = 8.8 Hz, 2H, Ph-H), 7.3 (d, J = 8.8 Hz, 2H, Ph-H) ppm. ^{13}C NMR ($CDCl_3$, 100 MHz): δ 43.8, 55.3, 73.0, 113.8, 118.2, 127.1, 134.6, 136.1, 159.0 ppm. IR (neat): 3404 (br, OH), 3075, 3002, 2934, 2836, 1640, 1612, 1586, 1514, 1464, 1442, 1302, 1248, 1175, 1106, 1036, 917, 872, 832, 768, 629, 586, 548 cm^{-1}.

5.6.2.2. Synthesis of 1-(4-Methoxyphenyl)-but-3-en-1-one. Oxidization of 1-(4-methoxyphenyl)-but-3-en-1-ol (15.6 g, 0.09 mol) with Jones reagent as described above gave 1-(4-methoxyphenyl)-but-3-en-1-one (4.3 g, 0.02 mol, 28% yield). ^{1}H NMR, ^{13}C NMR, and IR spectra match those reported in the literature.[57] ^{1}H NMR ($CDCl_3$, 400 MHz): δ 3.7 (d, J = 6.8 Hz, 2H, $-CH_2-$), 3.9 (s, 3H, $-OCHH_3$), 5.1−5.2 (m, 2H, $=CH_2$), 6.0−6.1 (m, 1H, =CH), 6.9 (d, J = 8.8 Hz, 2H, Ph-H), 8.0 (d, J = 8.8 Hz, 2H, Ph-H) ppm. IR (neat): 2841, 1676 (s, C=O), 1601, 1576, 1510, 1420, 1331, 1261, 1215, 1170, 1030, 912, 834, 733, 608 cm^{-1}.

*5.6.2.3. Synthesis of (1-(4-Methoxyphenyl)-but-2-en-1-one) **1b**.* Following the procedure described above 1-(4-methoxyphenyl)-but-3-en-1-one (4.3 g, 0.02 mol) resulted in **1b** (0.8 g, 4.60 mmol, 19% yield). The spectroscopic data of **1b** match those reported in the literature.[55,58] ^{1}H NMR ($CDCl_3$, 400 MHz): δ 2.0 (d, J = 6.0 Hz, 3H, $-CH_3$), 3.9 (s, 3H, $-OCHH_3$), 6.9−7.0 (m, 3H, =CH, Ph-H), 7.0−7.3 (m, 1H, =CH), 7.9 (d, J = 8.4 Hz, 2H, Ph-H) ppm. IR (neat): 2840, 1664 (s, C=O), 1618, 1598, 1507, 1440,1335, 1299, 1259, 1224, 1170, 1024, 963, 917, 809 cm^{-1}. GC/MS (EI): m/z: 176 (M^+), 161, 135 (100%), 107, 92, 77, 69.

*5.6.3. Preparation of **1c**. 5.6.3.1. Synthesis of 4-(1-Hydroxybut-3-enyl)benzonitrile.* Following the method described above 4-formylbenzonitrile (1.3 g, 0.01 mol) allyl bromide (1.5 g, 0.01 mol, 1.2 equiv) yield 4-(1-hydroxybut-3-enyl)benzonitrile in 77% yield (1.3 g, 7.70 mmol). ^{1}H NMR, ^{13}C NMR, and IR spectra match the reported literature.[52] ^{1}H NMR ($CDCl_3$, 400 MHz): δ 2.3 (s, 1H, −OH), 2.4−2.5 (m, 1H, $-CH_2$), 2.5−2.6 (m, 1H, $-CH_2$), 4.79−4.82 (m, 1H, −CH), 5.15−5.20 (m, 2H, $=CH_2$), 5.7−5.8 (m, 1H, =CH),7.5 (d, J = 8.4 Hz, 2H, Ph-H), 7.6 (d, J = 8.4 Hz, 2H, Ph-H) ppm. ^{13}C NMR ($CDCl_3$, 100 MHz): δ 43.8, 72.4, 111.2, 118.8, 119.5, 126.5, 132.2, 133. 4, 149.1 ppm. IR (neat): 3435 (br, OH), 3077, 3006, 2980, 2931, 2906, 2229 (s, C≡N), 1928, 1641, 1609, 1504, 1412, 1303, 1199, 1173, 1105, 1056, 1018, 999, 920, 873, 840, 760, 649, 630, 566 cm^{-1}.

5.6.3.2. Synthesis of 4-But-3-enoylbenzonitrile. Jones oxidation of 4-(1-hydroxybut-3-enyl)benzonitrile (1.3 g, 7.70 mmol) as described above yielded 4-but-3-enoylbenzonitrile (1.2 g, 7.00 mmol, 90% yield). ^{1}H NMR ($CDCl_3$, 400 MHz): δ 3.8 (d, J = 6.8 Hz, 2H, $-CH_2-$), 5.2−5.3 (m, 2H, $=CH_2$), 6.0−6.1 (m, 1H, =CH), 7.8 (d, J = 8.4 Hz, 2H, Ph-H), 8.0 (d, J = 8.4 Hz, 2H, Ph-H) ppm. ^{13}C NMR ($CDCl_3$, 100 MHz): δ 43.6, 116.5, 117. 9, 119.6, 128.7, 130.0, 132.6, 139.4 ppm. IR (neat): 3093, 3047, 2228 (s, C≡N), 1689 (s, C=O), 1645, 1606, 1566, 1425, 1406, 1394, 1335, 1291, 1210, 1177, 1108, 1009, 995, 936, 856, 834, 822, 769, 602, 574, 534 cm^{-1}. HRMS: m/z calculated for $C_{11}H_{10}NO^+$ $[M + H]^+$, 172.0762; found, 172.0762

*5.6.3.3. Synthesis of (E)-4-But-2-enoylbenzonitrile, **1c**.* 4-But-3-enoylbenzonitrile (1.2 g, 7.0 mmol) was converted to **1c** (0.9 g, 7.00 mmol, 77% yield) as described above. The ^{1}H NMR, ^{13}C NMR, and IR spectra of **1c** match those reported.[59] ^{1}H NMR ($CDCl_3$, 400 MHz): δ 2.0 (dd, J = 6.8 Hz, J = 1.2 Hz, 3H, $-CH_3$), 6.9 (dd, J = 15.4 Hz, J = 1.2 Hz, 1H, =CH), 7.1−7.2 (m, 1H, =CH), 7.8 (d, J = 8.4 Hz, 2H, Ph-H), 8.0 (d, J = 8.4 Hz, 2H, Ph-H) ppm. ^{13}C NMR ($CDCl_3$, 100 MHz): δ 18.8, 115.8, 118.0, 127.0, 128.9, 132.4, 141.2, 147.3, 189.4 ppm. IR (neat): 3095, 3048, 2972, 2914, 2850, 2231 (s, C≡N), 1672 (s, C=O), 1654, 1624 (s, C=C), 1560, 1442, 1405, 1375, 1332, 1293, 1220, 1177, 1107, 1073, 1040, 1017, 965 920, 864, 839, 809, 759, 663, 642, 567, 544 cm^{-1}. GC/MS (EI): m/z: 171(M^+), 156, 142, 130, 115, 102, 75, 69 (100%), 63, 51. HRMS: m/z calculated for $C_{11}H_9NONa^+$ $[M + Na]^+$,

194.05764; found, 194.05767; HRMS: m/z calculated for $C_{11}H_{10}NO^+$ $[M + H]^+$, 172.07571; found, 172.07569

5.7. Photolysis of 1a–c. *5.7.1. Product Studies of **1a** in Argon-Saturated $CDCl_3$.* A solution of **1a** (~20 mg, 137 μmol) in $CDCl_3$ (2 mL) was purged with argon and photolyzed via a Pyrex filter for 30 min at 298 K. ^1H NMR spectrum of the reaction mixture showed the formation of **2a** (33%), with 67% of remaining starting material. **2a**: ^1H NMR ($CDCl_3$, 400 MHz): δ 2.146 (dd, J = 7.2 Hz, J = 1.6 Hz, 3H, $-CH_3$), 6.399–6.481 (m, 1H, =CH), 6.827 (dd, J = 11.2 Hz, J = 1.6 Hz, 1H, =CH), 7.444–7.569 (m, 3H, Ph-H), 7.912–8.064 (m, 2H, Ph-H) ppm. GC/MS (EI): m/z 145 ($(M-H)^+$, 100%), 130, 116, 104, 77, 69, 50.

*5.7.2. Product Studies of **1a** in Oxygen-Saturated $CDCl_3$.* A solution of **1a** (~20 mg, 137 μmol) in $CDCl_3$ (2 mL) was purged with oxygen and photolyzed through a Pyrex filter for 30 min at 298 K. ^1H NMR analysis of the reaction mixture showed the formation of **2a** (26%), with 74% remaining starting material. The product was characterized by GC/MS chromatography.

*5.7.3. Product Studies of **1b** in Argon-Saturated $CDCl_3$.* A solution of **1b** (~20 mg, 114 μmol) in $CDCl_3$ (2 mL) was purged with argon and photolyzed via a Pyrex filter for 1.5 h at 298 K. ^1H NMR analysis of the reaction mixture showed the formation of **2b** (45%), with 55% remaining starting. The product was characterized by GC/MS chromatography and ^1H NMR spectroscopy of the reaction mixture. **2b**: ^1H NMR ($CDCl_3$, 400 MHz): δ 2.1 (dd, J = 7.2 Hz, J= 1.6 Hz, 3H, $-CH_3$), 3.9 (s, 3H, $-OCHH_3$), 6.35–6.40 (m, 1H, =CH), 6.8 (dd, J = 11.6 Hz, J= 1.6 Hz, 1H, =CH), 6.9–7.0 (m, 2H, Ph-H), 8.0 (d, J = 8.2 Hz, 2H, Ph-H) ppm. GC/MS (EI): m/z 176 (M^+), 161, 145, 135 (100%), 127, 115, 107, 92, 77, 69, 64.

*5.7.4. Product Studies of **1b** in Oxygen-Saturated $CDCl_3$.* A solution of **1b** (~20 mg, 114 μmol) in $CDCl_3$ (2 mL) was purged with oxygen and photolyzed through a Pyrex filter for 1.5 h at 298 K. ^1H NMR analysis of the reaction mixture showed the formation of **2b** (29%), 68% remaining starting material **1b** and 3% *p*-methoxybenzaldehyde. The product was characterized by GC-MS chromatography and ^1H NMR spectroscopy of the reaction mixture.

*5.7.5. Product Studies of **1c** in Argon-Saturated $CDCl_3$.* A solution of **1c** (~22 mg, 129 μmol) in $CDCl_3$ (2 mL) was purged with argon and photolyzed through a Pyrex filter for 1 h at 298 K. ^1H NMR spectrum of the reaction mixture showed the formation of **2c** (5%), with remaining starting material **1c** (95%). After 4 h, the product ratio increased to **2c** (11%) and **1c** (89%). The products were characterized by GC/MS chromatography and ^1H NMR spectroscopy of the reaction mixture. **2c**: ^1H NMR ($CDCl_3$, 400 MHz): δ 2.2 (dd, J = 7.2 Hz, J = 1.6 Hz, 3H, $-CH_3$), 6.5–6.6 (m, 1H, =CH), 6.9 (dd, J = 11.6 Hz, J = 1.6 Hz, 1H, =CH), 7.8 (d, J = 8.4 Hz, 2H, Ph-H), 8.0 (d, J = 8.4 Hz, 2H, Ph-H) ppm. ^{13}C NMR ($CDCl_3$, 100 MHz): δ 16.5, 115.8, 124.2, 128.7, 132.5, 132.6, 141.7, 146.7, 190.3 ppm. GC/MS (EI): m/z 171 (M^+, 100%), 156, 142, 130, 115, 102, 89, 75, 69, 63, 51. IR (neat): 3096, 3048, 2941, 2233 (C≡N), 1665 (C=O), 1612 (C=C), 1560, 1435, 1400, 1361, 1293, 1227, 1119, 1025, 1014, 914, 866, 831, 783, 732, 708, 644, 577, 544 cm^{-1}. HRMS: m/z calculated for $C_{11}H_9NONa^+$ $[M + Na]^+$, 194.05764; found, 194.05767; HRMS: m/z calculated for $C_{11}H_{10}NO^+$ $[M + H]^+$, 172.07571; found, 172.07569

*5.7.6. Product Studies of **1c** in Oxygen-Saturated $CDCl_3$.* A solution of **1c** (~20 mg, 117 μmol) in $CDCl_3$ (2 mL) was purged with oxygen and photolyzed through a Pyrex filter for 1 h at 298 K. ^1H NMR spectrum of the reaction mixture after 1 h showed the formation of **2c** (4%) and remaining starting material **1c** (96%). After 4 h of irradiation, the product ratio was decreased to **2c** (11%) and **1c** (89%).

■ ASSOCIATED CONTENT

Supporting Information

Cartesian coordinates and energies of **1**–**4**, IR, NMR, and MS spectra of **1** and **2** and the synthetic precursors to **1**, matrix isolation studies of **1b** and **1c**. This material is available free of charge via the Internet at http://pubs.acs.org.

■ AUTHOR INFORMATION

Corresponding Author

*A. D. Gudmundsdottir: e-mail, Anna.Gudmundsdottir@uc.edu; phone, 513-556-3380.

Notes

The authors declare no competing financial interest.

■ ACKNOWLEDGMENTS

This work was supported by NSF (CHE-1057481) and the Ohio Supercomputer Center. R.A.A.U.R. acknowledges a Harry B. Mark Fellowship from the Department of Chemistry, University of Cincinnati. R.L. and C.B. thank the Natural Sciences Research Council of Canada (NSERC) for financial support.

■ REFERENCES

(1) Dugave, C.; Demange, L. Cis-Trans Isomerization of Organic Molecules and Biomolecules: Implications and Applications. *Chem. Rev. (Washington, DC, U. S.)* **2003**, *103*, 2475–2532.

(2) Sankaranarayanan, J.; Muthukrishnan, S.; Gudmundsdottir, A. D. Photoremovable Protecting Groups based on Photoenolization. *Adv. Phys. Org. Chem.* **2009**, *43*, 39–77.

(3) Mulliken, R. S. The Excited States of Ethylene. *J. Chem. Phys.* **1979**, *71*, 556–557.

(4) Mulliken, R. S. The Excited States of Ethylene. *J. Chem. Phys.* **1976**, *66*, 2448–2451.

(5) Farmanara, P.; Stert, V.; Radloff, W. Ultrafast Internal Conversion and Fragmentation in Electronically Excited C_2H_4 and C_2H_3Cl Molecules. *Chem. Phys. Lett.* **1998**, *288*, 518–522.

(6) Mestdagh, J. M.; Visticot, J. P.; Elhanine, M.; Soep, B. Prereactive Evolution of Monoalkenes Excited in the 6 eV Region. *J. Chem. Phys.* **2000**, *113*, 237–248.

(7) Caldwell, R. A. Intersystem Corssing in Organic Photochemical Intermeidates. *Pure Appl. Chem.* **1984**, *56*, 1167–1177.

(8) Unett, D. J.; Caldwell, R. A. The Triplet State of Alkenes: Structure, Dynamics, Energetics and Chemistry. *Res. Chem. Intermed.* **1995**, *21*, 665–709.

(9) Caldwell, R. A.; Cao, C. V. Structural Effects on Twisted Olefin Triplet Lifetimes. Styrene Derivatives. *J. Am. Chem. Soc.* **1982**, *104*, 6174–6180.

(10) Caldwell, R. A.; Singh, M. Effect of a Polar Substituent on Olefin Triplet Lifetime. *J. Am. Chem. Soc.* **1983**, *105*, 5139–5140.

(11) Bonneau, R.; Herran, B. Structure and Properties of the Triplet State of Styrene Derivatives Studied by Laser-Flash-Photolysis. *Laser Chem.* **1984**, *4*, 151–170.

(12) Bonneau, R. Intersystem Crossing in Styrene and Styrene Derivatives. *J. Am. Chem. Soc.* **1982**, *104*, 2921–2923.

(13) Caldwell, R. A.; Cao, C. V. Lifetimes of Some Styrene Triplets in Fluid Solution. Triplet Geometries and the Effect of Alkylation. *J. Am. Chem. Soc.* **1981**, *103*, 3594–3595.

(14) Bonneau, R. The Perpendicular Triplet State of Ethylenic Compounds Observed by Nanosecond Laser Flash Photolysis. *J. Photochem.* **1981**, *17*, 24.

(15) Arai, T.; Tokumaru, K. Photochemical One-Way Adiabatic Isomerization of Aromatic Olefins. *Chem. Rev.* **1993**, *93*, 23−39.
(16) Lyons, A. L., Jr; Turro, N. J. Photophysics of Phenylcyclopropanes, Styrenes, and Benzocycloalkadienes. *J. Am. Chem. Soc.* **1978**, *100*, 3177−3181.
(17) Caldwell, R. A.; Cao, C. V. Structural Effects on Twisted Olefin Triplet Lifetimes. Styrene Derivatives. *J. Am. Chem. Soc.* **1982**, *104*, 6174−6180.
(18) Brede, O.; David, F.; Steenken, S. Styrene Triplets: Absorption Spectra, Lifetimes and Quantum Yields. *J. Photochem. Photobiol., A* **1996**, *97*, 127−131.
(19) García-Expósito, E.; González-Moreno, R.; Martín-Vilà, M.; Muray, E.; Bourdelande, J. L.; Branchadell, V.; Ortuño, R. M. On the Z−E Photoisomerization of Chiral 2-Pentenoate Esters: Stationary Irradiations, Laser-Flash Photolysis Studies, and Theoretical Calculations. *J. Org. Chem.* **2000**, *65*, 6958−6965.
(20) Misochko, E. Y.; Benderskii, V. A.; Goldschleger, A. U.; Akimov, A. V.; Shestakov, A. F. Formation of the CH_3-HF Complex in Reaction of Thermal F Atoms with CH_4 in Solid Ar. *J. Am. Chem. Soc.* **1995**, *117*, 11997−8.
(21) Caldwell, R. A.; Carlacci, L.; Doubleday, C. E., Jr.; Furlani, T. R.; King, H. F.; McIver, J. W., Jr. Viable Geometries for T_1-S_0 ISC in Alkene Triplets. *J. Am. Chem. Soc.* **1988**, *110*, 6901−3.
(22) Frisch, M. J.; Trucks, G. W.; Schlegel, H. B.; Scuseria, G. E.; Robb, M. A.; Cheeseman, J. R.; Scalmani, G.; Barone, V.; Mennucci, B.; Petersson, G. A.; et al., *Gaussian 09*, Revision B.01; Gaussian Inc.: Wallingford, CT, 2009.
(23) Becke, A. D. Density-Functional Thermochemistry. III. The Eole of Exact Exchange. *J. Chem. Phys.* **1993**, *98*, 5648−52.
(24) Phys. Rev. B: Condens. MatterLee, C.; Yang, W.; Parr, R. G. Development of the Colle-Salvetti Correlation-Energy Formula into a Functional of the Electron Density. *Phys. Rev. B: Condens. Matter* **1988**, *37*, 785−9.
(25) Muthukrishnan, S.; Mandel, S. M.; Hackett, J. C.; Singh, P. N. D.; Hadad, C. M.; Krause, J. A.; Gudmundsdóttir, A. D. Competition between α-Cleavage and Energy Transfer in α-Azidoacetophenones. *J. Org. Chem.* **2007**, *72*, 2757−2768.
(26) Muthukrishnan, S.; Sankaranarayanan, J.; Pace, T. C. S.; Konosonoks, A.; De Michiei, M. E.; Meese, M. J.; Bohne, C.; Gudmundsdottir, A. D. Effect of Alkyl Substituents on Photorelease from Butyrophenone Derivatives. *J. Org. Chem.* **2010**, *75*, 1393−1401.
(27) Upul Ranaweera, R. A. A.; Sankaranarayanan, J.; Casey, L.; Ault, B. S.; Gudmundsdottir, A. D. Triplet-Sensitized Photoreactivity of a Geminal Diazidoalkane. *J. Org. Chem.* **2011**, *76*, 8177−8188.
(28) Muthukrishnan, S.; Sankaranarayanan, J.; Klima, R. F.; Pace, T. C. S.; Bohne, C.; Gudmundsdottir, A. D. Intramolecular H-Atom Abstraction in γ-Azido-Butyrophenones: Formation of 1,5 Ketyl Iminyl Radicals. *Org. Lett.* **2009**, *11*, 2345−2348.
(29) Clark, W. D. K.; Steel, C. Photochemistry of 2,3-Diazabicyclo[2.2.2]oct-2-ene. *J. Am. Chem. Soc.* **1971**, *93*, 6347−6355.
(30) Lamola, A. A.; Mittal, J. P. Solution Photochemistry of Thymine and Uracil. *Science* **1966**, *154*, 1560−1561.
(31) Mitchell, R. H.; Bohne, C.; Wang, Y.; Bandyopadhyay, S.; Wozniak, C. B. Multistate π Switches: Synthesis and Photochemistry of a Molecule Containing Three Switchable Annelated Dihydropyrene Units. *J. Org. Chem.* **2005**, *71*, 327−336.
(32) Liao, Y.; Bohne, C. Alcohol Effect on Equilibrium Constants and Dissociation Dynamics of Xanthone−Cyclodextrin Complexes. *J. Phys. Chem.* **1996**, *100*, 734−743.
(33) Foresman, J. B.; Frisch, Æ. *Exploring Chemistry with Electronic Structure Methods*, 2nd ed.; Gaussian, Inc.: Pittsburgh, PA, 1996.
(34) Gonzalez, C.; Schlegel, H. B. An Improved Algorithm for Reaction Path Following. *J. Chem. Phys.* **1989**, *90*, 2154−2161.
(35) Gonzalez, C.; Schlegel, H. B. Reaction Path Following in Mass-Weighted Internal Coordinates. *J. Phys. Chem.* **1990**, *94*, 5523−5527.
(36) Labanowksi, J. K.; Andzelm, J. W. *Density Functional Methods in Chemistry*; Springer-Verlag: New York, 1991.
(37) Parr, R. G.; Weitao, Y. *Density Functional Theory in Atoms and Molecules*; Oxford University Press: Oxford, U.K., 1989.
(38) Bauernschmitt, R.; Ahlrichs, R. Treatment of Electronic Excitations within the Adiabatic Approximation of Time Dependent Density Functional Theory. *Chem. Phys. Lett.* **1996**, *256*, 454−464.
(39) Stratmann, R. E.; Scuseria, G. E.; Frisch, M. J. An Efficient Implementation of Time-Dependent Density-Functional Theory for the Calculation of Excitation Energies of Large Molecules. *J. Chem. Phys.* **1998**, *109*, 8218−8224.
(40) Foresman, J. B.; Head-Gordon, M.; Pople, J. A.; Frisch, M. J. Toward a Systematic Molecular Orbital Theory for Excited States. *J. Phys. Chem.* **1992**, *96*, 135−49.
(41) Tomasi, J.; Mennucci, B.; Cammi, R. Quantum Mechanical Continuum Solvation Models. *Chem. Rev.* **2005**, *105*, 2999−3093.
(42) Mennucci, B.; Cances, E.; Tomasi, J. Evaluation of Solvent Effects in Isotropic and Anisotropic Dielectrics and in Ionic Solutions with a Unified Integral Equation Method: Theoretical Bases, Computational Implementation, and Numerical Applications. *J. Phys. Chem. B* **1997**, *101*, 10506−10517.
(43) Cances, E.; Mennucci, B. Comment on "Reaction Field Treatment of Charge Penetration" [J. Chem. Phys. 112, 5558 (2000)]. *J. Chem. Phys.* **2001**, *114*, 4744−4745.
(44) Tomasi, J.; Persico, M. Molecular Interactions in Solution: An Overview of Methods Based on Continuous Distributions of the Solvent. *Chemical Reviews (Washington, D. C.)* **1994**, *94*, 2027−2094.
(45) Cramer, C. J.; Truhlar, D. G. Implicit Solvation Models: Equilibria, Structure, Spectra, and Dynamics. *Chemical Reviews (Washington, D. C.)* **1999**, *99*, 2161−2200.
(46) Iwata, K.; Hamaguchi, H. Construction of a Versatile Microsecond Time-Resolved Infrared Spectrometer. *Appl. Spectrosc.* **1990**, *44*, 1431−37.
(47) Yuzawa, T.; Kato, C.; George, M. W.; Hamaguchi, H. Nanosecond Time-resolved Infrared Spectroscopy with a Dispersive Scanning Spectrometer. *Appl. Spectrosc.* **1994**, *48*, 684−690.
(48) Wang, Y.; Yuzawa, T.; Hamaguchi, H.; Toscano, J. P. Time-Resolved IR Studies of 2-Naphthyl(carbomethoxy)carbene: Reactivity and Direct Experimental Estimate of the Singlet/Triplet Energy Gap. *J. Am. Chem. Soc.* **1999**, *121*, 2875−2882.
(49) Ault, B. S. Infrared Spectra of Argon Matrix-Isolated Alkali Halide Salt/Water Complexes. *J. Am. Chem. Soc.* **1978**, *100*, 2426−2433.
(50) El Bouakher, A.; Laborie, H.; Aadil, M.; El Hakmaoui, A.; Lazar, S.; Akssira, M.; Viaud-Massuard, M.-C. A Convenient Synthesis of New Pyrido[3,2-e][1,4]diazepine-2,5-diones and Pyrido[2,3-e][1,4]-diazepine-2,5-diones. *Tetrahedron Lett.* **2011**, *52*, 5077−5080.
(51) Bates, R. W.; Sridhar, S. A Synthesis of (−)-Mintlactone. *J. Org. Chem.* **2008**, *73*, 8104−8105.
(52) Guo, L.-N.; Gao, H.; Mayer, P.; Knochel, P. Preparation of Organoaluminum Reagents from Propargylic Bromides and Aluminum Activated by $PbCl_2$ and Their Regio- and Diastereoselective Addition to Carbonyl Derivatives. *Chem.—Eur. J.* **2010**, *16*, 9829−9834.
(53) Hathaway, S. J.; Paquette, L. A. Silanes in Organic Synthesis. 19. Examination of (−)-α-Naphthylphenylmethylallylsilane as a Template for Effecting Chirality Transfer from Silicon to Carbon. *J. Org. Chem.* **1983**, *48*, 3351−3353.
(54) Padwa, A.; Akiba, M.; Cohen, L. A.; MacDonald, J. G. Aza Cope Rearrangements in the Cyclopropenyl- and Allyl-Substituted Δ^2-Oxazolinone Systems. *J. Org. Chem.* **1983**, *48*, 695−703.
(55) Ochiai, M.; Yoshimura, A.; Mori, T.; Nishi, Y.; Hirobe, M. Difluoro-λ^3-Bromane-Induced Oxidative Carbon-Carbon Bond-Forming Reactions: Ethanol as an Electrophilic Partner and Alkynes as Nucleophiles. *J. Am. Chem. Soc.* **2008**, *130*, 3742−3743.
(56) Schneider, U.; Sugiura, M.; Kobayashi, S. Highly Selective Formation of Propargyl- and Allenyltrichlorosilanes and their Regiospecific Addition to Various Types of Aldehydes: Preparation of Both Allenic and Homopropargylic Alcohols. *Tetrahedron* **2006**, *62*, 496−502.
(57) Larock, R. C.; Lu, Y. D. Synthesis and Acylation of Allylic Mercuric Iodides: A Convenient Synthesis of Allylic Ketones. *J. Org. Chem.* **1993**, *58*, 2846−2850.

(58) Bisceglia, J. Á.; Díaz, J. E.; Torres, R. A.; Orelli, L. R. 1,n-Diamines. Part 3: Microwave-Assisted Synthesis of N-Acyl-N′-arylhexahydropyrimidines and Hexahydro-1,3-diazepines. *Tetrahedron Lett.* **2011**, *52*, 5238−5240.
(59) Manjolinho, F.; Grünberg, M. F.; Rodríguez, N.; Gooßen, L. J. Decarboxylative Allylation of Glyoxylic Acids with Diallyl Carbonate. *Eur. J. Org. Chem.* **2012**, 4680−4683.